Edge–Edge Interactions in Stacked Graphene Nanoplatelets

Eduardo Cruz-Silva,[†,‡,*] Xiaoting Jia,[§] Humberto Terrones,[⊥] Bobby G. Sumpter,[∥] Mauricio Terrones,[⊥,¶,△] Mildred S. Dresselhaus,[§,▼] and Vincent Meunier[‡]

[†]Department of Polymer Science and Engineering, University of Massachusetts, Amherst, Massachusetts 01003, United States, [‡]Department of Physics, Applied Physics, and Astronomy, Rensselaer Polytechnic Institute, Troy, New York 12180, United States, [§]Research Laboratory of Electronics, Massachusetts Institute of Technology, Cambridge, Massachusetts 02139, United States, [⊥]Department of Physics, 104 Davey Lab, The Pennsylvania State University, State College, Pennsylvania 16802, United States, [∥]Center for Nanophase Materials Science, and Computer Science and Mathematics Division, Oak Ridge National Laboratory, Oak Ridge, Tennessee 37831, United States, [¶]Department of Materials Science and Engineering & Center for 2-Dimensional and Layered Materials, The Pennsylvania State University, University Park, Pennsylvania 16802-6300, United States, [△]Research Center for Exotic Nanocarbons (JST), Shinshu University, Wakasato 4-17-1, Nagano 380-8553, Japan, and [▼]Department of Physics and Department of Electrical Engineering and Computer Science, Massachusetts Institute of Technology, Cambridge, Massachusetts 02139, United States

ABSTRACT High-resolution transmission electron microscopy studies show the dynamics of small graphene platelets on larger graphene layers. The platelets move nearly freely to eventually lock in at well-defined positions close to the edges of the larger underlying graphene sheet. While such movement is driven by a shallow potential energy surface described by an interplane interaction, the lock-in position occurs *via* edge–edge interactions of the platelet and the graphene surface located underneath. Here, we quantitatively study this behavior using van der Waals density functional calculations. Local interactions at the open edges are found to dictate stacking configurations that are different from Bernal (AB) stacking. These stacking configurations are known to be otherwise absent in edge-free two-dimensional graphene. The results explain the experimentally observed platelet dynamics and provide a detailed account of the new electronic properties of these combined systems.

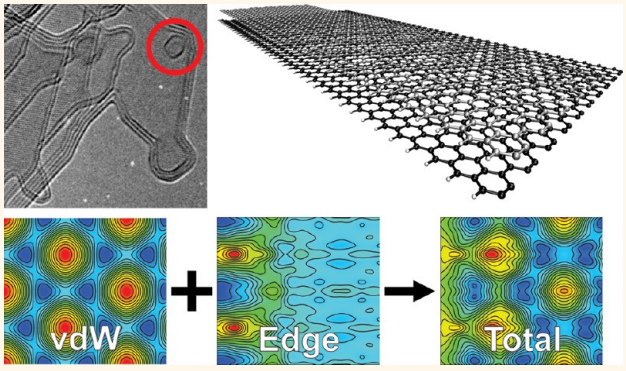

KEYWORDS: graphene nanoplatelets · graphene edges · stacking · density functional theory · diffusion

Since its experimental isolation,[1] graphene has attracted a great deal of attention as exemplified by the vast amount of work that predicted outstanding electronic properties in its two- and one-dimensional sheet and nanoribbon configurations.[2−5] Comprehensive reviews related to the electronic properties of graphene and graphene nanoribbons can be found in refs 6 and 7. In this context, theoretical and experimental research has contributed to establishing the expectations of graphene-based devices, and applications have been proposed as a potential replacement technology for silicon-based integrated nanoelectronic devices.[8] This includes the fabrication of transparent electrodes and electron collectors in solar cells,[9] an all-graphene semiconductor–metal–semiconductor junction,[10] and as a wide range of electronic, magnetic, and mechanical sensors,[11] among others.

While 2D graphene is a zero-gap semiconductor, the electronic properties of graphene nanoribbons (GNRs) are strongly influenced by their geometry and, in particular, by the shape of their edges.[4,5] In order for monolayer and few-layer graphene to realize their predicted potential in electronic device applications, it is imperative to control material variables such as the edge geometry and the number of layers. Recent reports have discussed experimental methods for reshaping the edges at the atomic scale, either by electron irradiation[12,13] or by Joule heating.[14] While controlling the edge geometry is clearly important for tailoring the electronic properties of graphene, other effects such as the stacking of the layers[15,16] and loop edge formation[17,18] could substantially modify the electronic properties. The methods used to post-process graphene and GNRs with rough edges often result in the formation

* Address correspondence to cruzsilvae@gmail.com.

Received for review January 25, 2013 and accepted February 14, 2013.

Published online February 14, 2013
10.1021/nn4004204

of unusual morphologies, such as small graphene platelets (as observed here) which "float" on other underlying graphene layers, similar to a puck floating on an air hockey table. It is noteworthy that the dynamics of such platelets constitute an unusual phenomenon since layer−layer interaction, which scales as the overlapping surface area, precludes the relative movement of the structure outside of their minimum energy position (*i.e.*, AB stacking).

It has been shown that the stacking of graphene not only can assist in tailoring the electronic properties of graphene[15,16] but it also modifies the binding interactions between carbon atoms. Experimental high-resolution transmission electron microscopy (HRTEM) and STM observations on graphene and GNR systems have demonstrated the presence of small graphene flakes that move nearly freely over larger graphene layers consisting of either large graphene patches or wide graphene nanoribbons.[19] While there is still a debate on whether these structures are indeed single-layered platelets or edgeless collapsed closed nanostructures,[20] in this work, we only consider the former nanostructures and the effect of edges on the interaction between stacked graphene platelets and larger subsurface sheets/plates. Figure 1a,b shows a small platelet of *ca.* 5 nm^2 that moves on top of a larger graphene plate. This small platelet is found to move along the edge of the base platelet and appears to become locked into positions where the platelet maximizes the edge overlap with the larger host plate located underneath.

In order to survey both the surface potential experienced by a graphene platelet while moving on top of a larger graphene sheet and the interaction potential between their edges, we constructed a molecular model consisting of a narrow GNR laying over a wider GNR, as illustrated in Figure 1c. The narrow GNR is then shifted along the *x* and *y* directions (as indicated in Figure 1d) to survey the variations in the electrostatic potential experienced by the narrow GNR when displaced on top of the underlying wider GNR. Since the employed model should represent a system in which the platelet size can vary, we used a GNR that is wide enough to remove all interactions between their own edges, thereby providing a faithful representation of the edge−edge interaction established between distinct graphene platelets and sheets, as shown in Figure 1a,b. It is also important to consider that the edges of zigzag nanoribbons are known to be stabilized following reconstruction into what the literature refers to as *reczag* edges (or 5-7 *reczag*), in which two edge hexagons transform into a heptagon/pentagon pair by a single bond rotation.[13,21] Our choice for zigzag (5-7 reczag) GNRs is 20z(rz) GNR (*ca.* 42 Å width) for the base and correspondingly 12z(rz) GNR (*ca.* 25 Å) for the platelet, while a 35aGNR (*ca.* 43 Å) base with a 21 aGNR (*ca.* 25 Å) platelet was chosen for the armchair

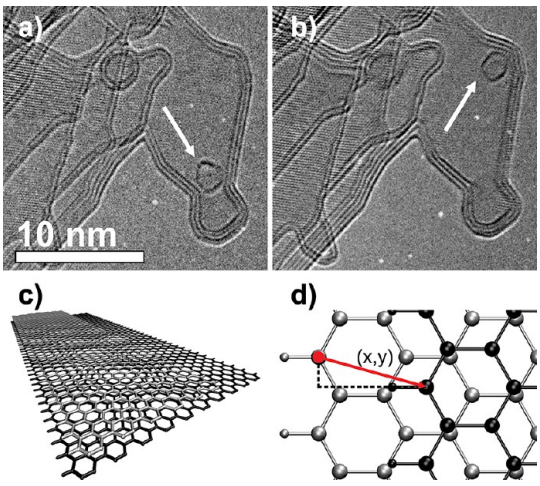

Figure 1. (a,b) High-resolution transmission electron micrographs of a graphene platelet (indicated by arrows) that moves along the edge of a larger graphene surface. (c,d) Ball-and-stick representation of the model used to calculate the edge−edge interactions of stacked graphene platelets. (c) Top graphene nanoribbon (gray) is displaced on top of a wider nanoribbon (black). (d) Displacement on *x* and *y* axes is measured relative to a perfect edge overlap, indicated by the arrow.

case for comparison. Given the symmetry of the system, the platelet GNR needs only to be moved from the edge to the center of the underlying GNR in the *x* (transverse) direction, while only one-half of the unit cell needs to be surveyed in the *y* (periodic) direction.

RESULTS AND DISCUSSION

First, we studied the stacking interactions of a zigzag edged graphene platelet on top of a GNR with the same edge geometry. In Figure 2a, we show the potential energy map as the zigzag edged platelet moves over the zigzag GNR. This energy map resembles the potential energy surface of a perfect graphene double layer (see Supporting Information, Figure S1), with the exception of the region where the edges are close to each other. The ground state (global minimum) and other local energy minima are marked by the letters A−G in Figure 2a. Unexpectedly, these metastable positions do not correspond to either AA or AB stacking but are positioned slightly off the AB stacking position by 0.25 Å. Figure 2b shows the potential profile across the lines located at y = 0.25 and y = 1.00 Å, which provides another way to examine these stable and metastable positions. While the ground state is located at E, the local minima at positions B, C, D, F, and G are nearly degenerate with E, having energy differences smaller than meV, *i.e.*, below the trusted accuracy of DFT. By subtracting the basal van der Waals interaction from the potential profile using graphene's potential energy profile (see Figures S1 and 2c), thereby highlighting the effect of edge−edge interactions, we observe that when edges are located beyond the first 2.5 Å, the bilayer graphene stacking potential dominates the interaction between the platelet

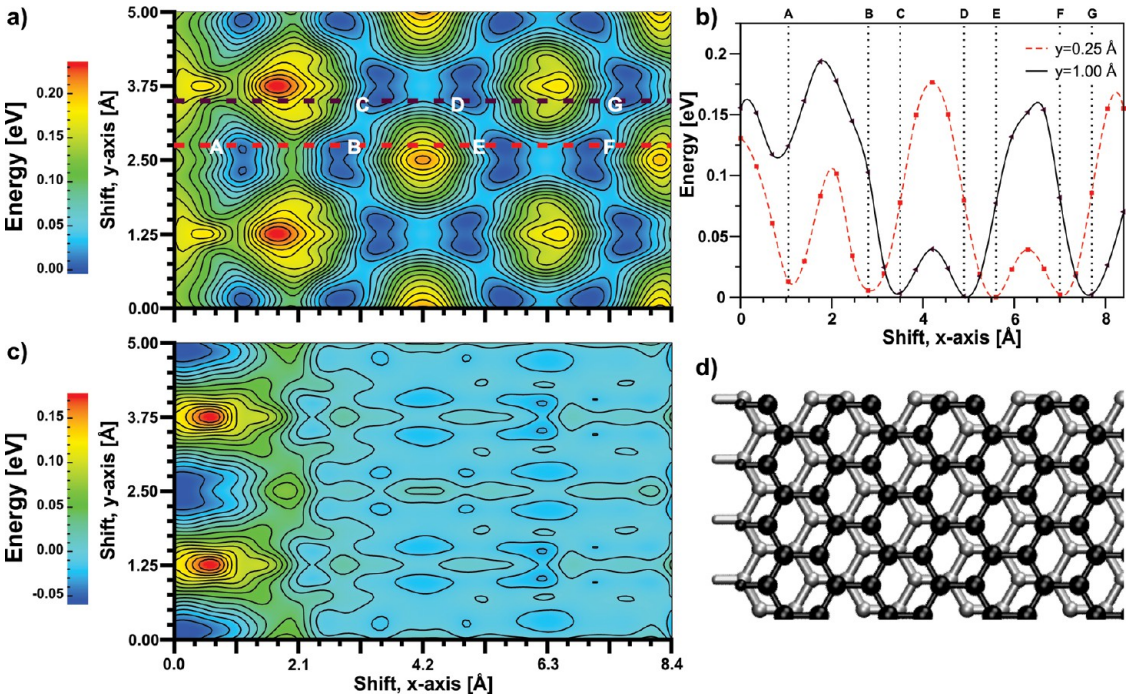

Figure 2. (a) Potential energy profile for a zigzag graphene nanoribbon moving on top of a wider graphene nanoribbon. The displacements are relative to a perfect AA stacking on the edge atoms and span 4 unit cells along the periodic direction *y* and 8.4 Å in the perpendicular *x* direction. (b) Potential line profile across *y* = 0.25 Å and *y* = 1.00 Å positions for stacked zigzag GNRs, which include the stable and metastable energy minima. (c) Potential energy profile for stacked two-dimensional bilayer graphene after the basal plane van der Waals interaction between these layers has been subtracted. (d) Ball-and-stick model for the metastable position A.

and the wider ribbon, and the deviations from the graphene van der Waals interaction are smaller than 0.05 eV per edge atom (2 meV/atom).

It is observed from the potential map shown in Figure 2c that the total potential is the sum of two competing interactions: one is the van der Waals interaction, which scales linearly with the overlapping area or number of atoms and favors AB stacking, while the second interaction occurs when the platelet is located closer to the edge of the underlying graphene layer, and it favors AA stacking. The diffusion of a graphene platelet when it is far from the base edge is hence dominated by the 2D graphene bilayer interaction, with an energy barrier of about 39 meV per platelet edge atom (1.7 meV/atom). When the distance between the edges is shorter than 2.5 Å, interactions between the localized edge states increase and create differences in total energy close to 0.18 eV. This, in turn, modifies the diffusion barrier near the edges and creates a metastable state in position A (Figure 2a,b,d) with an energy barrier of 96 meV per edge atom that traps the platelet at *ca.* 1.05 Å away from the base layer edge. Notice that the stacking configurations where the edges are aligned (x = 0.0 Å) are all unfavorable, and that the least favorable position is the AA stacking closest to the edge alignment. The final stable and metastable positions are therefore a trade-off between these two interactions.

Turning to the pentagon−heptagon reconstructed edges on zigzag graphene nanoribbons (rzGNR), we observed two different cases for AA stacking, with either aligned (AA) or opposing (AA*) pentagons and heptagons. The potential energy map shown in Figure 3a indicates that the overlapping edges with AA* stacking display the most unfavorable configuration. We can also observe the presence of several near-degenerate local minima, which are examined in detail in the energy profiles of Figure 3b. The metastable positions located at C, D, E, E*, F, F*, and G (where a starred position means the platelet is aligned with an AA* stacking at the edge) have very similar energies, and the energy barriers to move from one position to another are even lower than those for the zigzag case, oscillating between 7.5 and 25 meV per edge atom (0.3 to 1 meV/atom). However, the ground state is located at the B position (x = 2.45 Å), which is also slightly off AA stacking by 0.35 Å, providing an alignment of the edge atoms, as shown in Figure 3d. There is another metastable position located at the A* point, which has an asymmetric barrier of 30/7 meV per edge atom (1.25/0.3 meV/atom), making it less probable to be populated.

Figure 3c shows the interaction potential after subtracting the basal interlayer van der Waals interaction, as was done for the zigzag system. We observed that while the movement of the smaller plate is still largely dominated by the basal van der Waals interaction when it is far from the base edge, the reconstruction of the platelet edge modifies the interaction. In this case, we indeed observe that an armchair edge moves on top of a zigzag

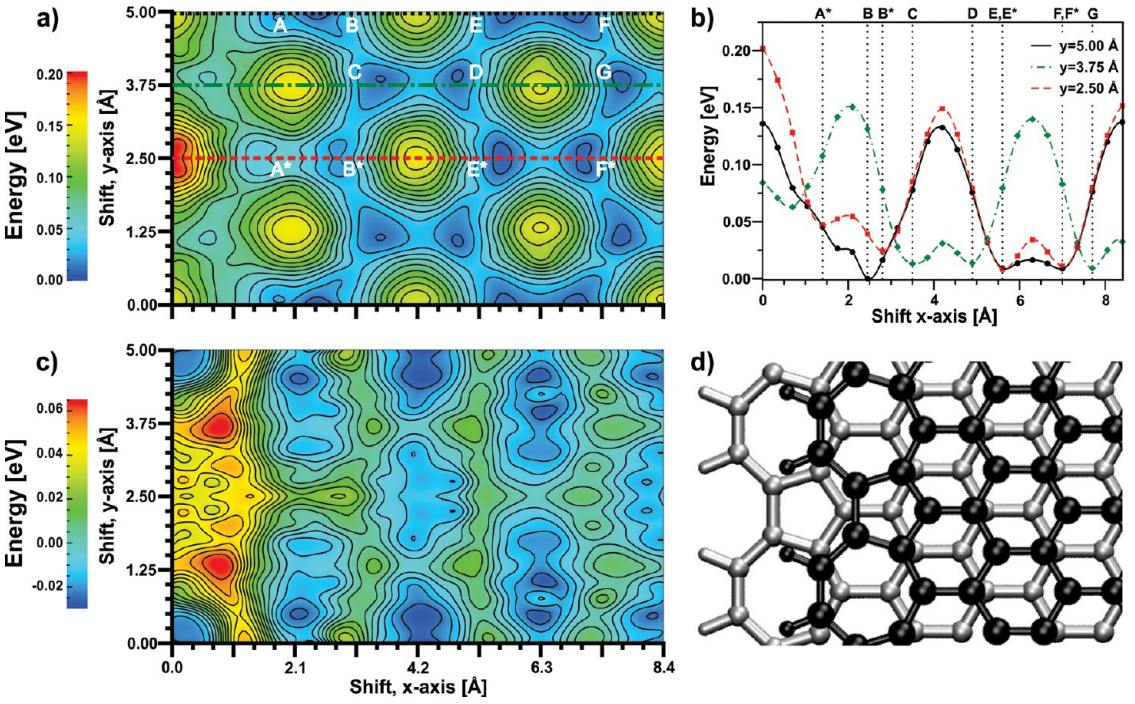

Figure 3. (a) Potential energy profile for a (5,7) reczag graphene nanoribbon moving on top of a wider nanoribbon with the same edge geometry. The displacements are relative to a perfect AA stacking on the edge atoms, and span 2 unit cells along the periodic direction *y* and 8.4 Å in the perpendicular *x* direction. (b) Potential line profile across *y* = 5.0, *y* = 3.75, and *y* = 2.5 Å positions for stacked reczag GNRs. (c) Potential energy profile for the same system after the basal plane van der Waals interactions between these layers has been subtracted. (d) Ball-and-stick model for the stable position B.

oriented surface, as reflected in the more uneven topography of the potential energy surface beyond 3.0 Å when compared to the zigzag case shown in Figure 2c.

We also performed the analysis of the interaction with the armchair edges. Armchair GNRs show a similar behavior compared to stacked graphene bilayers (Figure 4a,b), with stacking energy variations when the edges of the nanoribbons are closer than 2 Å. The metastable states exhibit diffusion barriers below 20 meV per edge atom (1 meV/atom), with the exception of the ground state C, which presents a barrier of about 45 meV per edge atom in order to move to neighboring stable states B and D, and a barrier of 20 meV to the mirror-symmetric C state. This state occurs when the edges of the GNRs are 2.5 Å apart from each other and very close to AB stacking, as shown in Figure 4b.

The previous findings allow us to clearly identify the most stable stacking positions of the platelet and the graphene sheet, in the presence of edge−edge interactions. In order to facilitate comparison with experiments, we have simulated the HRTEM images corresponding to these positions. Figure 5b,c shows the simulated HRTEM views of the most stable states for 5-7 reczag and armchair edges based on our nanoplatelet model, located at 2.45 and 2.5 Å. For zigzag edges, we choose the metastable state located at 1.05 Å from the edge, as illustrated in Figure 5a. It is observed that, while the platelet edge is easily discernible in both the reczag and the armchair cases, it is more difficult to identify for the zigzag case, probably due to the short edge−edge distance when compared to the other two cases.

Turning our attention to the electronic properties of these systems, our calculations demonstrate that armchair edges (Figure 6a) always result in a nonmagnetic ground state, where the bands are basically a superposition of those of its components. For 5-7 reconstructed zigzag edges (Figure 6b,c), the model system shows that, while the bands are mostly a superposition of those of the base and the top plate, there is some clear mixing of states close to the Fermi energy for the minority carriers, and the total magnetic moment is 0.09 μ_B per edge atom.

For zigzag edges (Figure 7a,b), we observed that, for the energies beyond the ±1.5 eV window, energy bands were essentially a superposition of those of the base and the plate systems. However, within this energy range, the bands are affected by the presence of a significant interaction between the localized edge states in these zigzag nanoribbons. For the isolated components, electronic states are localized around the zigzag edges on the base (edges α,γ) and the platelet (β,δ). As it can be observed on the isosurface plot of the wave functions of these bands (Figure 7c,d), the interaction between these localized states at the common edge (α,β) results in the formation of a covalent bond between these, with a bonding state ($\alpha\beta$, with a maximum between the edges, as shown in Figure 7c) and an antibonding state ($\alpha\beta$*, with a node between the edges; see Figure 7d). With the formation of bonding and antibonding states between edges (α,β), these now share the same spin configuration.

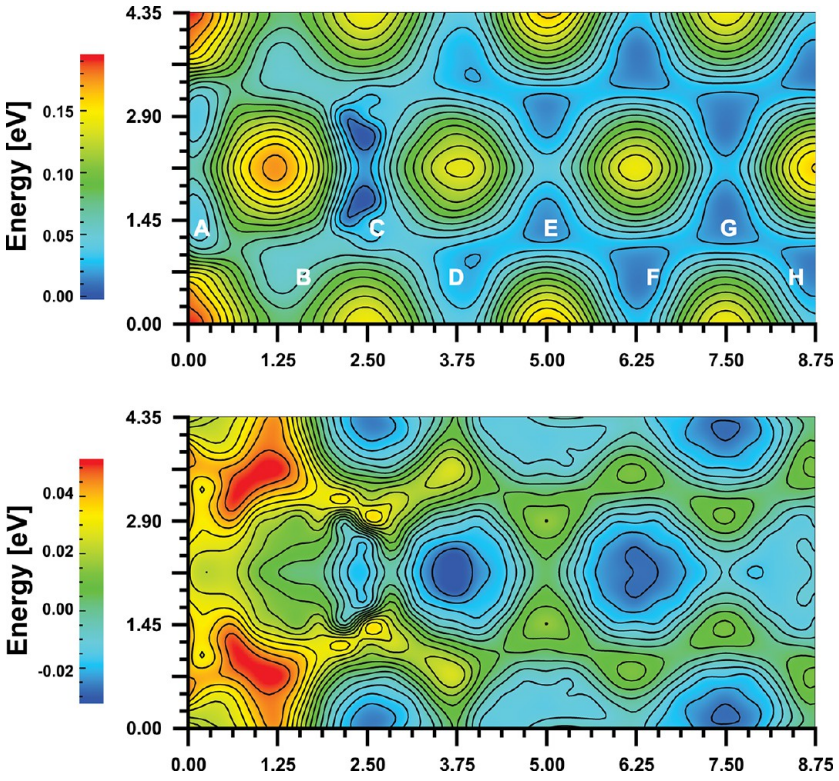

Figure 4. Electrostatic potential profile for an armchair graphene nanoribbon moving on top of a wider graphene nanoribbon. The displacements are relative to a perfect AA stacking on the edge atoms and span 1 unit cell along the periodic direction *y* and 8.4 Å in the perpendicular *x* direction. The bottom image shows the electrostatic profile after the basal van der Waals interaction for stacked graphene has been subtracted.

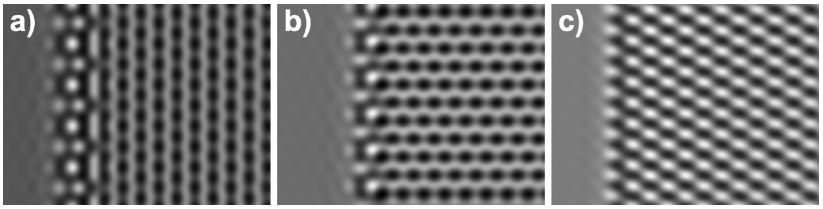

Figure 5. High-resolution electron microscopy simulation of the stable and metastable structures found within this study. (a) Metastable zigzag nanoribbon edges. (b) Simulation for the (5,7) reczag case. (c) Simulation of the armchair stacked ribbons.

To preserve the antiferromagnetic order expected in isolated GNRs, edges (γ,δ) now must also share their spin configuration, which results in a total magnetic moment of 0.75 μ_B per edge atom.

In order to understand the dynamics of the diffusion and to determine the associated length and time scales, we estimated the mobility of a graphene flake moving on top of a larger graphene layer by using the adiabatic trajectory method, in which the platelet diffuses on the surface with small hops between neighboring energy minima.[22] The model for the thermal diffusion of an adatom on a crystal surface is used, where a rigid graphene platelet will be the moving object. We will start with a graphene platelet with only armchair and zigzag edges, where all edges are far from the base layer edges (*i.e.*, over 2.5 Å), such that all surface dynamics are dominated by van der Waals interactions.

By thermal excitation, the graphene platelet can gain enough energy to overcome the energy barrier (E_B) and hop to a neighboring stable state. Assuming a random walk model, the mean square displacement after time t is $L = a(\nu t)^{1/2}$, where ν is the hopping frequency, a is the hopping distance, and t is the elapsed time. According to the Arrhenius law, the hopping frequency is expressed as $\nu = \nu_0 \exp(-E_B/k_BT)$, where ν_0 is the vibrational frequency of the adatom at the absorption site, k_B is the Boltzmann constant, and T is the temperature, and the hopping time is $\tau = 1/\nu = \tau_0 \exp(E_B/k_BT)$, with $\tau_0 = 1/\nu_0$. From this, we can find an expression for the diffusion time in terms of the energy barrier and the diffusion length $t = (L^2/a^2)\tau_0 \exp(E_B/k_BT)$. The diffusion coefficient D is defined as $D = a^2/z\tau = 1/3a^2\nu_0 \exp(E_B/k_BT)$, where $z = 3$ is the number of nearest neighbors of the honeycomb lattice.

The rigid graphene platelet vibrational frequency can be calculated from the electrostatic potential profile as $\nu_0 = 1/2\pi(k/m)^{1/2}$, where $k = -dF/dx = d^2E/dx^2$.

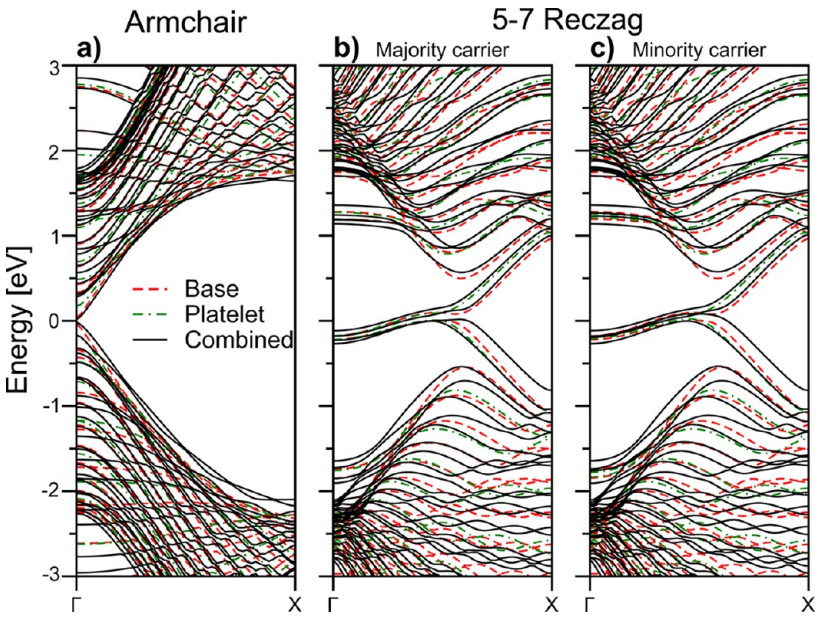

Figure 6. Comparison of the electronic band structures for the stacked graphene bilayer at the edge-locking positions for armchair and 5-7 reczag edges. (a) Armchair GNR always develops a paramagnetic ground state, and the bands are mostly a superposition of the components. (b) Majority and (c) minority carriers band structure for 5-7 reczag GNRs, which shows a weakly spin-polarized ground state with a slight mixing of the states of the component ribbons when combined.

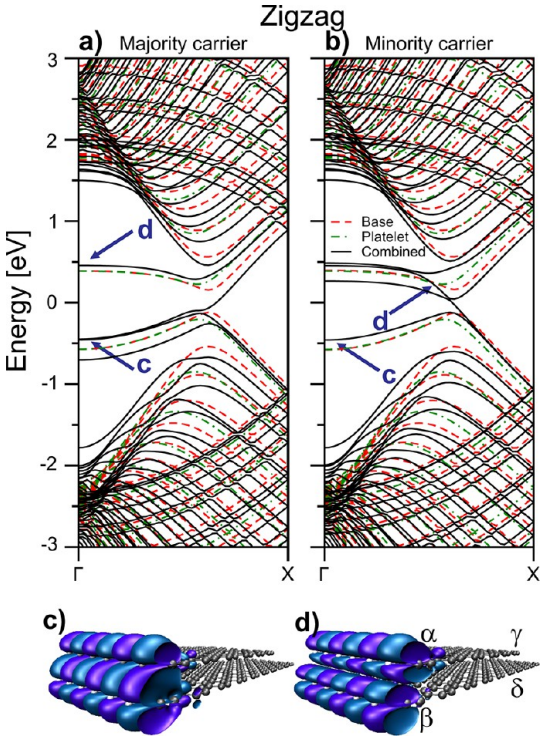

Figure 7. (a,b) Band structure of stacked zigzag graphene nanoribbons at their metastable position A shown in Figure 2a. The arrows point to the bands resulting from the mixing of the edge states of the base and the platelet into a bonding (c) and an antibonding (d) state. (c,d) Isosurfaces of the wavefunctions have been plotted at values = ±0.05 Å$^{-3/2}$.

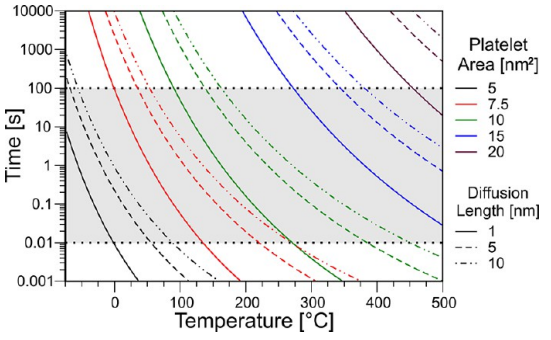

Figure 8. Temperature dependence of the excursion times for graphene platelets of different sizes and for different excursion lengths. The shaded area represents the time scales that could be experimentally relevant for observation under the electron microscope.

Given that both E and m have a linear dependency on the number of atoms in the system, ν_0 has a constant value of $\nu_0 = 6.018 \times 10^{11}$ Hz, as calculated from the potential shown in Figure S1 of the Supporting Information. We can also see that the energy barrier E_B scales with the surface area of the platelet, and hence, it also has a linear dependence with the system size. The plot shown in Figure 8 depicts the excursion time as a function of temperature for selected excursion lengths and platelet sizes. The plot confirms that the computed time scales for a platelet to move across the graphene basal plane are well within the range of time-resolved HRTEM imaging.

While the model used here implies that graphene nanoplatelets diffuse only by rigid translations preserving AB stacking, recent experimental observations have found that diffusion can also occur through a different pathway that includes the rotation of the graphene

platelets into noncommensurate stacking configurations with relative orientation angles different from multiples of 60°.[19] This rotation causes the translational potential energy landscape to flatten[16] and hence allows for a very fast diffusion even at low temperatures, corresponding to a superlubric state.[19] Previous DFT-based studies using the local density approximation (LDA) found the rotational barrier to be on the order of 4 meV per atom.[23] Since LDA is known to overestimate binding energies, we can assume this to be an upper bound. In this case, a nanoplatelet of similar size to that of Figure 1 should require an excitation energy on the order of 0.9 eV to enter into this superlubric state, which is beyond thermal excitation energies, but well within the range of excitations caused by the 200 keV electron beam in HRTEM observations. This analysis lends further support to the interpretation of a hockey-puck-type platelet motion on a quasi-frictionless "iced surface". While a puck moves because it receives energy from a hockey stick, these platelets move because both thermal energy and electronic excitations caused by the electron beam result in lattice vibrations that give the platelet enough energy to hop across potential barriers.

CONCLUSIONS

We have demonstrated that graphene platelets moving over larger graphene layers will diffuse similar to 2D graphene until diffusion brings the edges of neighboring layers closer than 3.0 Å. At this point, the interaction between the edges will create both stable and metastable states that lock the platelet to a fixed distance of the base plate edge and away from the most stable AB stacking. This distance is *ca.* 1 Å for zigzag edges and *ca.* 2.5 Å for both the armchair and the 5-7 reconstructed zigzag edges. As the platelet grows in size, it is expected that van der Waals interactions will overcome the interaction between the edges and full AB stacking will be reached. Analysis of the electronic structure shows that, in the case of zigzag edges, the strong localization of the edge states coupled with the close distance results in the formation of bonding and antibonding states. This result indicates that the stacking interactions of small graphene platelets could cause important modifications in the local environment of larger graphene plates, thus causing unexpected behaviors such as the limiting of the epitaxial growth of a platelet or arresting the reconstruction of an edge during combined Joule heating and electron irradiation experiments. Measurements of the shifts in position at stacked graphene layers, in combination with surface diffraction techniques, could make it possible to discern whether or not the observed stacked graphene has zigzag or 5-7 reczag edges.

COMPUTATIONAL METHODS

In order to accurately describe the interactions between stacking graphene layers, calculations were performed using the revision 367 (trunk-367) of the development version of the SIESTA code,[24] which incorporates the van der Waals exchange-correlation functional of Dion *et al.*[25] as implemented by Roman-Perez and Soler.[26] A double-ζ numerical pseudoatomic orbital basis set with polarization orbitals, a real-space mesh for the electrostatic potential integration equivalent to a plane wave energy cutoff of 250 Ry, and a gamma point centered Monkhorst-Pack sampling lattice with 8 k-points along the periodic direction were employed. These conditions were found to yield good numerical convergence. Electronic structure calculations were performed using a spin-polarized Hamiltonian. In order to survey the electrostatic potential in positions out of equilibrium, the atomic positions were fixed in the *xy* plane, while atoms were allowed to relax in the *z* (normal) direction until the forces are smaller than 0.04 eV/Å. HRTEM simulations of the relevant structures were also performed using the SimulaTEM program.[27]

Conflict of Interest: The authors declare no competing financial interest.

Acknowledgment. E.C.S. was supported in part by PHaSE, an Energy Frontier Research Center funded by the U.S. DOE under Award No. DE-SC0001087. X.J. acknowledges ONR, N00014-09-1-1063, for support. M.S.D. acknowledges NSF/DMR 1004147. M.T. acknowledges JST-Japan for funding the Research Center for Exotic NanoCarbons, under the Japanese regional Innovation Strategy Program by the Excellence. M.T. also thanks support from a Penn State Center for Nanoscale Science Seed grant on 2-D Layered Materials (DMR-0820404). B.G.S. acknowledges support from the Center for Nanophase Materials Sciences (CNMS), sponsored at Oak Ridge National Laboratory by the Scientific User Facilities Division, U.S. Department of Energy. Research at RPI (VM) was also sponsored in part by the Army Research Laboratory and was accomplished under Cooperative Agreement Number W911NF-12-2-0023.

Supporting Information Available: The electrostatic potential surface of 2D graphene is presented in Figure S1. This material is available free of charge *via* the Internet at http://pubs.acs.org.

REFERENCES AND NOTES

1. Novoselov, K. S.; Geim, A. K.; Morozov, S. V.; Jiang, D.; Zhang, Y.; Dubonos, S. V.; Grigorieva, I. V.; Firsov, A. A. Electric Field Effect in Atomically Thin Carbon Films. *Science* **2004**, *306*, 666–669.
2. Wallace, P. R. The Band Theory of Graphite. *Phys. Rev.* **1947**, *71*, 622–634.
3. Dresselhaus, M. S.; Dresselhaus, G. Intercalation Compounds of Graphite. *Adv. Phys.* **2002**, *51*, 1–186.
4. Nakada, K.; Fujita, M.; Dresselhaus, G.; Dresselhaus, M. S. Edge State in Graphene Ribbons: Nanometer Size Effect and Edge Shape Dependence. *Phys. Rev. B* **1996**, *54*, 17954–17961.
5. Miyamoto, Y.; Nakada, K.; Fujita, M. First-Principles Study of Edge States of H-Terminated Graphitic Ribbons. *Phys. Rev. B* **1999**, *59*, 9858–9861.
6. Castro Neto, A. H.; Guinea, F.; Peres, N. M. R.; Novoselov, K. S.; Geim, A. K. The Electronic Properties of Graphene. *Rev. Mod. Phys.* **2009**, *81*, 109–162.
7. Terrones, M.; Botello-Méndez, A. R.; Campos-Delgado, J.; López-Urías, F.; Vega-Cantú, Y. I.; Rodríguez-Macías, F. J.; Elías, A. L.; Muñoz-Sandoval, E.; Cano-Márquez, A. G.; Charlier, J.-C.; *et al.* Graphene and Graphite Nanoribbons: Morphology, Properties, Synthesis, Defects and Applications. *Nano Today* **2010**, *5*, 351–372.

8. Kim, K.; Choi, J.-Y.; Kim, T.; Cho, S.-H.; Chung, H.-J. A Role for Graphene in Silicon-Based Semiconductor Devices. *Nature* **2011**, *479*, 338–344.
9. Zhu, Y.; Sun, Z.; Yan, Z.; Jin, Z.; Tour, J. M. Rational Design of Hybrid Graphene Films for High-Performance Transparent Electrodes. *ACS Nano* **2011**, *5*, 6472–6479.
10. Hicks, J.; Tejeda, A.; Taleb-Ibrahimi, A.; Nevius, M. S.; Wang, F.; Shepperd, K.; Palmer, J.; Bertran, F.; Fèvre, P. L.; Kunc, J.; *et al.* A Wide-Bandgap Metal–Semiconductor–Metal Nanostructure Made Entirely from Graphene. *Nat. Phys.* **2013**, *9*, 49–54.
11. Hill, E. W.; Vijayaragahvan, A.; Novoselov, K. Graphene Sensors. *IEEE Sens. J.* **2011**, *11*, 3161–3170.
12. Girit, Ç. Ö.; Meyer, J. C.; Erni, R.; Rossell, M. D.; Kisielowski, C.; Yang, L.; Park, C.-H.; Crommie, M. F.; Cohen, M. L.; Louie, S. G.; *et al.* Graphene at the Edge: Stability and Dynamics. *Science* **2009**, *323*, 1705–1708.
13. Koskinen, P.; Malola, S.; Häkkinen, H. Evidence for Graphene Edges beyond Zigzag and Armchair. *Phys. Rev. B* **2009**, *80*, 073401.
14. Jia, X.; Hofmann, M.; Meunier, V.; Sumpter, B. G.; Campos-Delgado, J.; Romo-Herrera, J. M.; Son, H.; Hsieh, Y.-P.; Reina, A.; Kong, J.; *et al.* Controlled Formation of Sharp Zigzag and Armchair Edges in Graphitic Nanoribbons. *Science* **2009**, *323*, 1701–1705.
15. Bao, W.; Jing, L.; Velasco, J., Jr.; Lee, Y.; Liu, G.; Tran, D.; Standley, B.; Aykol, M.; Cronin, S. B.; Smirnov, D.; *et al.* Stacking-Dependent Band Gap and Quantum Transport in Trilayer Graphene. *Nat. Phys.* **2011**, *7*, 948–952.
16. Shibuta, Y.; Elliott, J. A. Interaction between two Graphene Sheets with a Turbostratic Orientational Relationship. *Chem. Phys. Lett.* **2011**, *512*, 146–150.
17. Jia, X.; Campos-Delgado, J.; Gracia-Espino, E. E.; Hofmann, M.; Muramatsu, H.; Kim, Y. A.; Hayashi, T.; Endo, M.; Kong, J.; Terrones, M.; *et al.* Loop Formation in Graphitic Nanoribbon Edges Using Furnace Heating or Joule Heating. *J. Vac. Sci. Technol., B* **2009**, *27*, 1996–2002.
18. Cruz-Silva, E.; Botello-Méndez, A. R.; Barnett, Z. M.; Jia, X.; Dresselhaus, M. S.; Terrones, H.; Terrones, M.; Sumpter, B. G.; Meunier, V. Controlling Edge Morphology in Graphene Layers Using Electron Irradiation: From Sharp Atomic Edges to Coalesced Layers Forming Loops. *Phys. Rev. Lett.* **2010**, *105*, 045501.
19. Feng, X.; Kwon, S.; Park, J. Y.; Salmeron, M. Superlubric Sliding of Graphene Nanoflakes on Graphene. *ACS Nano* **2013**, 10.1021/nn305722d.
20. Harris, P. J. F. Hollow Structures with Bilayer Graphene Walls. *Carbon* **2012**, *50*, 3195–3199.
21. Koskinen, P.; Malola, S.; Häkkinen, H. Self-Passivating Edge Reconstructions of Graphene. *Phys. Rev. Lett.* **2008**, *101*, 115502.
22. Antczak, G.; Ehrlich, G. Jump Processes in Surface Diffusion. *Surf. Sci. Rep* **2007**, *62*, 39–61.
23. Lebedeva, I. V.; Knizhnik, A. A.; Popov, A. M.; Ershova, O. V.; Lozovik, Y. E.; Potapkin, B. V. Fast Diffusion of a Graphene Flake on a Graphene Layer. *Phys. Rev. B* **2010**, *82*, 155460.
24. Soler, J. M.; Artacho, E.; Gale, J. D.; García, A.; Junquera, J.; Ordejón, P.; Sánchez-Portal, D. The SIESTA Method for *Ab Initio* Order-N Materials Simulation. *J. Phys.: Condens. Matter* **2002**, *14*, 2745–2779.
25. Dion, M.; Rydberg, H.; Schröder, E.; Langreth, D. C.; Lundqvist, B. I. van der Waals Density Functional for General Geometries. *Phys. Rev. Lett.* **2004**, *92*, 246401.
26. Román-Pérez, G.; Soler, J. M. Efficient Implementation of a van der Waals Density Functional: Application to Double-Wall Carbon Nanotubes. *Phys. Rev. Lett.* **2009**, *103*, 096102.
27. Gómez-Rodríguez, A.; Beltrán-del-Río, L. M.; Herrera-Becerra, R. SimulaTEM: Multislice Simulations for General Objects. *Ultramicroscopy* **2010**, *110*, 95–104.